

RSC Advances



This is an *Accepted Manuscript*, which has been through the Royal Society of Chemistry peer review process and has been accepted for publication.

Accepted Manuscripts are published online shortly after acceptance, before technical editing, formatting and proof reading. Using this free service, authors can make their results available to the community, in citable form, before we publish the edited article. This *Accepted Manuscript* will be replaced by the edited, formatted and paginated article as soon as this is available.

You can find more information about *Accepted Manuscripts* in the [Information for Authors](#).

Please note that technical editing may introduce minor changes to the text and/or graphics, which may alter content. The journal's standard [Terms & Conditions](#) and the [Ethical guidelines](#) still apply. In no event shall the Royal Society of Chemistry be held responsible for any errors or omissions in this *Accepted Manuscript* or any consequences arising from the use of any information it contains.



Journal Name

ARTICLE TYPE

Cite this: DOI: 10.1039/xxxxxxxxxx

Photostability of thermally-hydrosilylated silicon quantum dots

Jeslin J Wu^{*a} and Uwe R Kortshagen^{*a}Received Date
Accepted Date

DOI: 10.1039/xxxxxxxxxx

www.rsc.org/journalname

The photostability of luminescent silicon quantum dots is critical for optoelectronic and photovoltaic applications. While nanocrystals synthesized in a nonthermal plasma and thermally hydrosilylated with dodecyl groups exhibit quantum yields exceeding 60 %, their optical properties degrade with UV exposure. A 20 % (absolute) reduction in quantum yield was observed within 4 h of UV irradiation. The origin of instability was identified to stem from unpaired electrons generated at the nanocrystal surface as a result of the breaking of silicon hydride bonds. Recovery of the nanocrystals' quantum yield can be achieved by passivating the dangling bonds generated during photobleaching. Moreover, no degradation in optical properties was observed with further UV irradiation, indicating that photostable silicon nanocrystals were synthesized.

1 Introduction

Since the observation of photoluminescence from porous silicon in 1990¹, the appeal of silicon in optoelectronic and biological devices and in third generation photovoltaics has grown. At the nanoscale, silicon exhibits size-dependent optical and electronic properties, which allows the tailoring of their band gap and emission wavelengths. Silicon quantum dots (SiQDs) were applied in hybrid nanocrystal-organic LEDs by Cheng *et al.* Peak external quantum efficiencies up to 8.6 % were attained for LEDs emitting from red to near-infrared.² In photovoltaic applications, silicon nanocrystal (SiNC) layers functioning as luminescent downshifters have led to enhancements in the internal quantum efficiencies of solar cells.^{3,4} Recently, carrier multiplication studies have demonstrated the possibility of further increasing solar cell efficiencies past the Shockley Queisser limit.^{5,6}

To be a promising candidate for the abovementioned applications, the SiQDs must exhibit enhanced optical properties and stability with environmental exposure. Mangolini *et al.* obtained photoluminescence quantum yields (PLQY) exceeding 60 % from SiNCs synthesized in a nonthermal plasma reactor and thermally hydrosilylated with organic ligands, specifically, 1-dodecene.⁷ The hydrosilylated NCs can be colloiddally dispersed into organic solvents for solution-phase device fabrication. However, alkyl functionalized silicon surfaces are prone to oxidation⁸, and their photoluminescence has been shown to degrade with prolonged UV exposure.^{8–10}

In order to fabricate photostable SiNCs, it is necessary to understand the origin of the photodegradation. Here, we study the stability of hydrosilylated, nonthermal plasma-synthesized SiQDs under 365-nm light. Photoluminescence measurements of colloidal SiQDs indicate degradation of the QDs' PLQY with irradiation time. Electron paramagnetic resonance (EPR) and Fourier transform infrared spectrometry (FT-IR) are used to probe the origin of the photodegradation; the results revealed an increase in dangling bond defects due to the breakage of silicon hydride bonds at the NC surface. The passivation of these dangling bonds in a second hydrosilylation reaction led to the recovery of the QDs' PLQY. Furthermore, the resulting SiQDs were photostable, and no further degradation in PLQY was observed with additional UV exposure.

^a Department of Mechanical Engineering, University of Minnesota, Minneapolis, MN, USA 55455. E-mail: jeslinwu@umn.edu, kortshagen@umn.edu. Tel: +1 612-625-4028

† Electronic Supplementary Information (ESI) available: XRD spectrum and TEM image of SiNCs (S1). Emission spectra of the as-produced, UV irradiated, and rehydrosilylated SiNCs (S2). Time evolution of IR absorbance of CH_x and SiH_x groups during in-situ photobleaching on ATR crystal (S3). FT-IR spectra of the SiH_x deformation modes of as-produced and UV-irradiated SiNCs and a deconvoluted spectrum (S4). Typical FT-IR spectra and deconvoluted SiH_x stretching modes of H-terminated and thermally-hydrosilylated SiNCs (S5). Deconvolution procedure of SiH_x stretching modes (S6). See DOI: 10.1039/b000000x/

2 Experimental

Silicon nanocrystals 4.2 nm in size were prepared using a non-thermal plasma reactor in a process that was previously reported.¹¹ Argon and silane (5 % in helium) were flown into a flow-through reactor at 35 sccm and 13 sccm, respectively. The reactor pressure was maintained at 1.4 Torr using a butterfly valve. Dissociation of the silane was achieved using a non-thermal plasma that was excited by a 13.56 MHz radio-frequency power source. 100 sccm of hydrogen was injected into the afterglow of the synthesis plasma to passivate the SiNCs' surface, and the resulting hydrogen-terminated SiNCs were collected on a stainless steel mesh downstream of the plasma.

Post synthesis, Si-H bonds on the SiNCs' surface were partially replaced by stable Si-C bonds via a thermal hydrosilylation process using 1-dodecene (96 %) in a background solvent of mesitylene (98+ %). The collected SiQDs (~ 10 mg), along with the stainless steel mesh, were placed in a degassed mixture of the alkene (4 ml) and mesitylene (20 ml), and the solution was sonicated for 1 min to disperse the NCs. The resulting suspension was transferred into a glass boiling flask for the thermal hydrosilylation reaction and placed in a sand bath that was heated to 215 °C for over 3 h. A cold water condenser was used to prevent solvent evaporation. The resulting SiNC colloid was filtered through a 0.2 μm PTFE filter to remove agglomerates of unreacted NCs. Subsequently, the NCs were dried in a stream of nitrogen under vacuum prior to analysis.

Unwanted organic polymers formed during the thermal hydrosilylation process were removed by washing the SiNCs. Dried SiNCs were re-dispersed in 1 ml of toluene (99 %) and precipitated in 14 ml of acetonitrile (99.8+ %). Subsequently, the precipitated solution was sonicated and centrifuged at 4500 rpm. Finally, the supernatant was removed, and the process was repeated several times. All processes were performed in nitrogen atmosphere, and all solvents were degassed prior to usage.

To mimic sunlight in the UV spectrum under AM1.5G conditions, a 100 W mercury vapor lamp coupled with a 365-nm filter was used. SiQDs dispersed in toluene at a concentration of 5 mg/ml were exposed to 365-nm light at a power density of ~ 4 mW/cm² for a duration of up to 24 h for the photostability study. The irradiation was conducted in either vacuum or nitrogen atmosphere.

The nanocrystal size and crystallinity were determined via X-ray diffraction (XRD) and transmission electron microscopy (TEM). XRD was performed using a Bruker-AXS Microdiffractometer with 2.2 kW sealed Cu X-ray source, and Debye-Scherrer fits of the integrated XRD patterns were used to determine the average SiNC size. The SiNCs were imaged using a FEI Technai T12 transmission electron microscope equipped with an energy-dispersive X-ray spectroscopy system. SiNCs dispersed in toluene were drop cast onto a borosilicate glass and lacey carbon TEM

grid, and placed under vacuum for 1 h to ensure solvent evaporation prior to analysis.

The surface chemistry of the SiNCs were analyzed using Fourier transform infrared spectroscopy (FT-IR). FT-IR measurements were performed on a Bruker ALPHA FT-IR spectrometer using the ATR single reflection module in a nitrogen-filled glovebox. SiNCs dispersed in toluene were drop cast onto the diamond ATR crystal and allowed to dry. Time study of species desorption from the QD surface was performed by irradiating the drop-cast SiNC film with a 365-nm UV light. Measurements were acquired at 15-min intervals for over 16 h. Fitting of the FT-IR spectra was performed using Voigt distributions. By fixing the position of the absorption peaks and their FWHM, time evolution of the absorption intensities of the individual peaks was obtained. The coefficients of determination, R², were used to determine quality of fits; all fits possessed R² values above 0.99.

Photoluminescence of SiQDs was measured using an Ocean Optics USB2000 spectrometer and integrating sphere setup whose absolute spectral response was calibrated using an Ocean Optics LS-1-CAL tungsten halogen light source. The validity of the calibration was verified using the fluorescence standard, Rhodamine 101 inner salt dispersed in ethanol. Photoluminescence was measured by irradiating SiQDs dispersed in 0.6 ml of toluene at a concentration of ~ 1 mg/ml with a 395-nm LED.

Electron paramagnetic resonance (EPR) was used to probe the density of unpaired electrons at the NC surface. 5 mg of hydrosilylated, UV irradiated, and re-hydrosilylated SiQDs dispersed in 0.1 ml of toluene were added to three 5 mm diameter borosilicate glass tubes. The EPR measurements were performed at room temperature using Bruker Continuous Wave EleXsys E500 EPR spectrometer equipped with a X-band (9 GHz) microwave bridge and a spherical Super High-Q (SHQ) resonator. Measurements were acquired at a microwave attenuation of 30 dB. The field was centered at 3339 G with a sweep width of 100 G. A modulation frequency of 100 kHz and amplitude of 1 G were used. The time constant and conversion time were set at 40.96 ms.

3 Results & discussion

Silicon nanocrystals were synthesized in a nonthermal plasma reactor and functionalized with 1-dodecene via thermal hydrosilylation reaction that has been described by Mangolini *et al.*¹² A typical X-ray diffraction (XRD) pattern of these SiNCs is shown in Figure S1 in the Supporting Information. Debye-Scherrer fits of XRD peaks established an average particle size of ~ 4.2 nm. The PLQY of these as produced QDs dispersed in toluene was measured to be 56 ± 6 % with peak wavelength at 828 ± 3 nm, which corresponds to band gap emission of the SiQDs.¹³

The photostability of the QDs to UV exposure was studied by irradiating colloidal NCs sealed in nitrogen atmosphere with 365-nm light at a power density that is comparable to that of sunlight

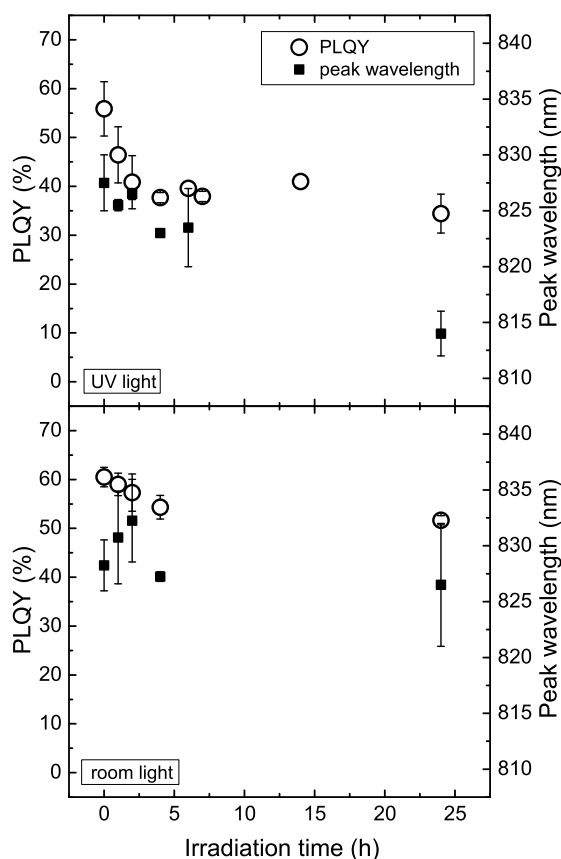


Fig. 1 Time-study of SiQDs' PLQY (open circles) and peak PL wavelength (solid squares) during UV light exposure (top). The SiQDs' photoluminescence under room light is shown for comparison (bottom).

in the UV region under AM1.5G conditions. This was calculated to be equivalent to $\sim 4 \text{ mW/cm}^2$. Figure 1 reveals that the UV irradiation resulted in significant degradation of the SiQDs' optical properties. Within 4 h of irradiation, their PLQY degraded from $\sim 56 \%$ to less than 40% —almost 20% decrease in the QDs' PLQY. After 4 h of irradiation, steady-state was reached and no further degradation was observed. In comparison, under room (fluorescent) light, only slight ($< 5 \%$) PLQY degradation was observed. Insignificant change in the photoluminescence peak wavelength was detected (see Figure S2 in Supporting Information), aside from a blueshift at 24 h of UV irradiation that is most likely the result of oxidation. The increased oxidation is indicative of the photo-induced enhanced oxidation rate that has been reported by several groups.^{14,15}

Photo-induced degradation was also observed in hydrogenated amorphous silicon (a-Si:H) due to a mechanism known as the Staebler-Wronski effect (SWE). It was shown that prolonged light illumination leads to a decrease in photoconductivity of a-Si:H

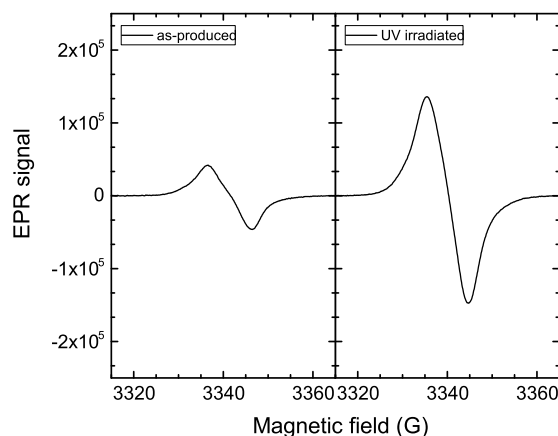


Fig. 2 EPR spectra of SiNCs before and after UV exposure.

films^{16–18}, which is attributed to the creation of defects from the breakage of Si-H or Si-Si bonds.¹⁹ UV light is also known to break surface bonds of flat and porous silicon during photochemical hydrosilylation reactions. In this process, it is believed that high-energy photons are able to homolytically cleave silicon hydride bonds to generate reactive sites for the attachment of organic ligands.^{20,21}

Unpaired electrons generated by the abovementioned process can be probed via electron paramagnetic (or spin) resonance (EPR).^{22–24} The EPR of nonthermal plasma-produced SiNCs has been studied extensively by Pereira *et al.*^{22,23} Two defect signals have been detected in freestanding SiNCs: (1) *D* centers allocated to three-fold coordinated silicon (or dangling bonds) in a disordered environment, and (2) an asymmetrical signal assigned to *P_b* centers at the interface of the SiNC and its oxide shell. A typical EPR signal of hydrosilylated SiNCs is shown in Figure 2. The spectrum resembles that of SiNCs with low initial defect density (LIDD) shown in Reference [23] and exhibits an insignificant *P_b* signal. For these LIDD SiNCs, the dangling bond density has been calculated to be less than 1 per 200 NCs.

The EPR of UV-irradiated SiNCs revealed a significantly higher density of unpaired electrons (Figure 2). These unpaired electrons can act as sites for electron-hole recombination, preventing radiative recombination, thus, resulting in a reduction in the SiQDs' PLQY.^{25,26} Due to the lack of asymmetry, the bulk of the EPR signal amplification is attributed to an increase in *D* centers that is the result of the generation of dangling bonds due to bond breakage, similar to results reported by Dersch *et al.*¹⁹

The approximately 3.5 times increase in dangling bond defect density may not explain the 20% reduction in PLQY. Recently, it has been presented that if the energy of the photon were above that of the work function of the SiNC's surface, an electron can be ejected from the conduction band, leaving a re-

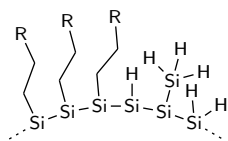


Fig. 3 Hydrosilylated surface of SiNCs.

active cation species at the surface.^{27,28} These positively-charged species can act as exciton traps, preventing electron-hole recombination. However, since cations are not EPR active, another method will need to be employed for the detection of these defects (not in the scope of this work).

Two material properties are proposed to play critical roles in the SWE observed in a-Si:H films: (1) disorder in the silicon network and (2) the presence of hydrogen.²⁹ These are also characteristics of the SiNC surface; thus, the elevated *D* center signal is postulated to be derived from unpaired electrons at the NC surface.

At 4.2 nm, almost 50 % of the silicon atoms in a SiNC lie on its surface.³⁰ FT-IR spectroscopy reveals that the surface of non-thermal plasma-produced SiNCs is highly disordered, comprising of hydrogen in the form of SiH₃, along with SiH and SiH₂, as depicted in Figure 3. Steric factors limit the coverage with long alkyl ligands on the silicon surface to ~ 50 %.³¹ A typical IR spectrum of 1-dodecene functionalized SiNCs is represented by Figure 4. Peaks between 3000 cm⁻¹ and 2800 cm⁻¹ are fingerprints of CH_x stretching modes from the dodecyl groups; their deformation modes absorb between 1500 cm⁻¹ and 1200 cm⁻¹. No CH_x vibrational modes were observed from the unfunctionalized SiNCs (Figure 4). This indicates that the carbon on the functionalized SiNC surface originate from the organic ligands—not contaminates from the synthesis process.

Significant coverage with hydrogen is present on the SiNC surface before and after hydrosilylation (Figure 4). The triplet between 2200 cm⁻¹ and 2000 cm⁻¹ are characteristic SiH_x stretching modes. A deconvoluted spectrum of the SiH_x mode of the thermally-hydrosilylated SiNCs is shown in the inset of the figure. The peak at ~ 2130 cm⁻¹ is assigned to the SiH₃, and the SiH₂ and SiH modes appear at ~ 2097 cm⁻¹ and ~ 2070 cm⁻¹, respectively. Due to the proximity and overlap of the symmetrical and asymmetrical modes, their peaks have been grouped in this study. The deformation modes of the SiH_x groups are visible between 1000 cm⁻¹ and 800 cm⁻¹.³² The broad Si-O-Si peak between 1100 cm⁻¹ and 1000 cm⁻¹ indicates slight oxidation. Since insignificant Si-O-Si absorbance was observed in the unfunctionalized SiNCs, it is deduced that the oxidation occurred during the hydrosilylation reaction as a result of impurities in the nitrogen gas and/or solvents that were used.

Through FT-IR spectroscopy, it is possible to study changes in the surface chemistry of the SiNCs due to photobleaching. Hy-

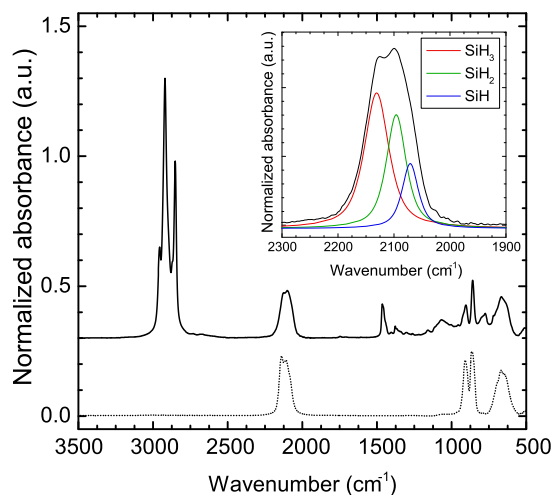


Fig. 4 Typical FT-IR spectra of H-terminated SiNCs (dotted line) and thermally-hydrosilylated SiNCs (solid line). Inset shows deconvoluted spectra of the silicon hydride stretching modes of hydrosilylated SiNCs: SiH₃ (red), SiH₂ (green) and SiH (blue).

dro-silylated SiNCs were drop cast onto a diamond attenuated total reflectance (ATR) crystal and exposed to 365-nm light for up to 16 h. FT-IR spectra measured at 15-min intervals revealed the stability of alkyl ligands, or Si-C bonds, against UV irradiation (see Figure S3 in Supporting Information); on the other hand, the coverage with silicon hydrides on the NC surface decreased with irradiation time. Unfortunately, due to the high absorptivity of silicon in the UV region, only a few monolayers of the SiNC film were exposed to the UV light, and an accurate fraction of hydrides cleaved from the surface could not be obtained from the data. However, knowing the stability of the dodecyl groups on the SiNC surface, FT-IR spectra of SiNCs irradiated *ex-situ* can be normalized to the total absorbance of the CH_x stretching modes.

SiNCs from the photoluminescence stability tests were drop cast onto the ATR crystal for FT-IR measurements. Figure 5 shows the IR absorbance of SiH_x stretching modes of the hydrosilylated SiNCs before and after UV irradiation (normalized to the integrated CH_x absorbance). The normalized data indicated ~ 20 % decrease in the total SiH_x absorption intensity (Figure 6). The desorption of silicon hydrides can also be observed in the SiH_x deformation modes in the IR (see Figure S4 in Supporting Information). Deconvolution of the SiH_x stretching modes (Figure 6) reveals ~ 8 – 10 % reductions in both SiH₃ and SiH₂ groups after UV exposure; insignificant changes in the SiH absorption intensity was observed. These results are similar to thermal desorption experiments wherein the weaker SiH₃ groups were the first to desorb from the surface, followed by SiH₂ groups, and the SiH groups remained the most tightly bound to the NC.^{33–35} Ther-

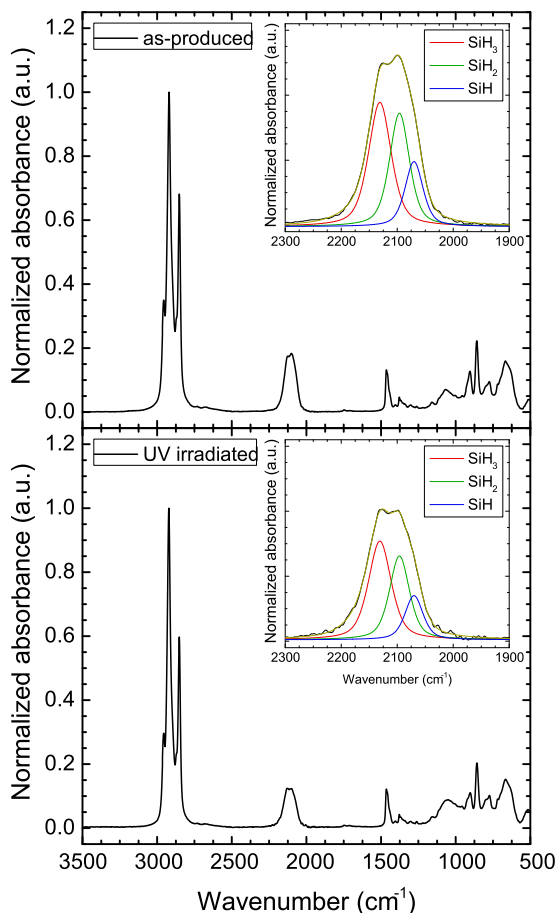
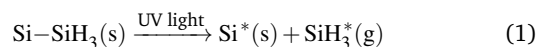


Fig. 5 FT-IR spectra of SiNCs before (top) and after UV irradiation (bottom). Insets show deconvoluted FT-IR spectra of SiH₃ (red), SiH₂ (green), and SiH (blue) modes.

mal hydrosilylation of nonthermal plasma-synthesized, hydrogen-terminated SiNCs also proceed favorably via the SiH₃ group^{36,37} (see Figure S5 in Supporting Information). The PLQY steady-state reached at 4 h (Figure 1) represents the point at which all the weaker bonds susceptible to UV cleavage were removed from the surface.

SiH₃ groups are bound to the surface via a single Si-Si bond. The Si-Si bond, with a bond strength of 2.0 – 2.7 eV³⁵, is one of the weaker bonds on the NC surface; thus, 365-nm (3.4 eV) light has sufficient energy to homolytically cleave the Si-Si bond, yielding a volatile SiH₃ specie that desorbs from the NC.^{26,38} The desorption reaction can be represented as:



where (s) and (g) denote surface species and species in the gas phase, respectively, and superscript * denotes a surface dangling

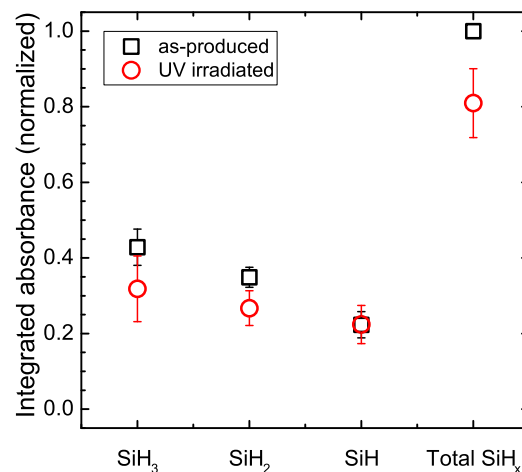
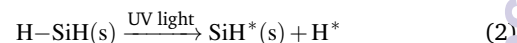


Fig. 6 Integrated IR absorbance of silicon hydride stretching modes before and after UV irradiation.

bond.

SiH₂ groups are doubly bonded to the silicon surface, and the strength of the Si-H bond is estimated to be ~ 3.67 eV³⁴; thus, desorption of the SiH₂ groups seems less likely. However, steric interactions between neighboring SiH₃ and SiH₂ groups generate strain on the NC surface, weakening bonds.³⁹ Gupta *et al.* estimate the Si-H bond in the SiH₂ group on an Si(100)-(2×1) surface to be ~ 3.19 eV.³⁴ These weakened bonds are, therefore, more susceptible to bond cleavage by the 3.4 eV light via the following process:



The resulting increase in SiH may be offset by the reaction of the highly mobile monatomic hydrogen^{40,41} with a neighboring silicon hydride group to form hydrogen gas (H₂) that is desorbed from the surface. Hydrogen desorption in the form of H₂ was also observed by Pusek *et al.* in time-of-flight (TOF) analysis of the desorption products of silicon surfaces irradiated with a vacuum ultraviolet laser (VUV).⁴²

With the understanding that the instability of SiQDs under UV light is a result of the generation of dangling bonds at the NC surface, we propose new pathway to create photostable SiQDs. Hydrosilylation is a well-established method for the passivation of silicon surfaces²⁰ and is a technique that can be employed for the passivation of the dangling bonds generated during photobleaching. EPR shows a decrease in unpaired electron density at the SiNCs surface by heating photobleached SiNCs above 150 °C in the presence of 1-dodecene (Figure 7). With 0.1 ml of 1-dodecene per 5 mg of SiNCs, an ~ 25 % decrease in EPR signal was observed; with 0.5 ml of 1-dodecene, over 60 % reduction in EPR

signal was observed. In the latter case, sufficient 1-dodecene was present to passivate the majority of the surface defects, nearly restoring the EPR signal to the initial (as-produced) intensity.

Passivation of the surface defects through the second hydrosilylation reaction also led to complete recovery of the photobleached SiQDs' photoluminescence (Figure 8). It should be noted that in the absence of 1-dodecene, heating of the SiNCs showed no recovery. This implies the recovery mechanism is dissimilar to the silicon network restructuring proposed for the healing of SWE defects in a-Si:H via thermal annealing.²⁹

Interestingly, further UV irradiation of the re-hydrosilylated SiNCs displayed no further degradation (Figure 8). This implies that the weaker bonds that are susceptible to the 365-nm light had been removed during the first UV exposure; the remaining surface is thus photostable. However, while the SiNCs are stable under 365-nm light, it is possible that exposure to light with energy greater than 3.4 eV will still result in photodegradation.

4 Conclusions

The photostability of thermally-hydrosilylated SiNCs produced in a nonthermal plasma has been studied. 365-nm light with a power density similar to that of the UV spectrum in AM1.5G sun was used as the irradiation source. UV irradiation resulted in ~ 20 % (absolute) decrease in the SiQDs' PLQY, reaching a saturation of ~ 40 % within 4 h. Similar to the SWE in a-Si:H, photodegradation was found to be a result of the creation of dangling bonds due to the breaking of silicon hydride bonds at the SiNC surface. These dangling bonds act as centers for nonradiative recombination, resulting in the deterioration of the SiNCs' optical properties. The results demonstrate the inability of thermal hydrosilylation to remove the weaker silicon hydride bonds that are susceptible to UV cleavage. However, the PLQY of the photobleached SiNCs can be recovered via thermal hydrosilylation post UV irradiation. The resulting SiNCs are photostable and do not degrade under further irradiation. The photodegradation and recovery process is summarized in Figure 9.

5 Acknowledgements

This work was supported primarily by the MRSEC Program of the National Science Foundation under grant DMR-1420013. Parts of this work were carried out in the College of Science and Engineering Characterization Facility, University of Minnesota, which receives partial support from NSF through the NNIN program. NMR spectroscopy reported in this work was supported by the Office of the Director, National Institutes of Health under Award Number S10OD011952.

References

- 1 L. T. Canham, *Appl. Phys. Lett.*, 1990, **57**, 1046 – 1048.
- 2 K.-Y. Cheng, R. Anthony, U. R. Kortshagen and R. J. Holmes, *Nano Lett.*, 2011, **11**, 1952 – 1956.
- 3 V. Svrcek, A. Slaoui and J.-C. Muller, *Thin Solid Films*, 2004, **451 - 452**, 384 – 388.
- 4 Z. Yuan, G. Pucker, A. Marconi, F. Sgrignuoli, A. Anopchenko, Y. Jestin, L. Ferrario, P. Bellutti and L. Pavesi, *Sol. Energy Mater. Sol. Cells*, 2011, **95**, 1224 – 1227.
- 5 D. Timmerman, J. Valenta, K. Dohnalova, W. D. A. M. de Boer and T. Gregorkiewicz, *Nat. Nanotechnol.*, 2011, **167**, 1 – 4.
- 6 M. T. Trinh, R. Limpens, W. D. A. M. de Boer, J. M. Schins, L. D. A. Siebbeles and T. Gregorkiewicz, *Nat. Photonics*, 2012, **6**, 316 – 321.
- 7 D. Jurbergs, E. Rogojina, L. Mangolini and U. Kortshagen, *Appl. Phys. Lett.*, 2006, **88**, 233116.
- 8 S. Godefroo, M. Hayne, M. Jivanescu, A. Stesmans, M. Zacharias, O. I. Lebedev, G. Van Tendeloo and V. V. Moshchalkov, *Nat. Nanotechnol.*, 2008, **3**, 174 – 178.
- 9 K. Pettigrew, Q. Liu, P. Philip and S. Kauzlarich, *Chem. Mater.*, 2003, **15**, 4005 – 4011.
- 10 J. Yang, R. Liptak, D. Rowe, J. Wu, J. Casey, D. Witker, S. A. Campbell and U. Kortshagen, *Appl. Surf. Sci.*, 2014, **323**, 54 – 58.
- 11 L. Mangolini, E. Thimsen and U. Kortshagen, *Nano Lett.*, 2005, **5**, 655 – 659.
- 12 L. Mangolini, D. Jurbergs, E. Rogojina and U. Kortshagen, *Phys. Status Solidi*, 2006, **3**, 3975 – 3978.
- 13 M. Wolkin, J. Jorne, P. Fauchet, G. Allan and C. Delerue, *Phys. Rev. Lett.*, 1999, **82**, 197 – 200.
- 14 M. A. Tischler, R. T. Collins, J. H. Stathis and J. C. Tsang, *Appl. Phys. Lett.*, 1992, **60**, 639 – 641.
- 15 J. Harper, *Langmuir*, 1997, **13**, 4652 – 4658.
- 16 M. Stutzmann, W. Jackson and C. Tsai, *Phys. Rev. B*, 1985, **32**, 32 – 47.
- 17 H. Fritzsche, *Solid State Commun.*, 1995, **94**, 953 – 955.
- 18 H. Fritzsche, *Annu. Rev. Mater. Res.*, 2001, **31**, 47 – 79.
- 19 H. Dersch, *Appl. Phys. Lett.*, 1981, **38**, 456 – 458.
- 20 J. M. Buriak, *Chem. Rev.*, 2002, **102**, 1271 – 1308.
- 21 J. M. Buriak, *Chem. Mater.*, 2014, **26**, 763 – 772.
- 22 R. Pereira, D. Rowe, R. Anthony and U. Kortshagen, *Phys. Rev. B*, 2011, **83**, 155327.
- 23 R. N. Pereira, D. J. Rowe, R. J. Anthony and U. Kortshagen, *Phys. Rev. B*, 2012, **86**, 085449.
- 24 D. Pierreux and A. Stesmans, *Phys. Rev. B*, 2002, **66**, 165320.
- 25 C. Delerue, G. Allan and M. Lannoo, *Phys. Rev. B*, 1993, **48**, 24 – 48.
- 26 G. Allan, C. Delerue and M. Lannoo, *Phys. Rev. Lett.*, 1996, **76**, 2961 – 2964.
- 27 X. Wang, R. E. Ruther, J. A. Streifer and R. J. Hamers, *J. Am.*

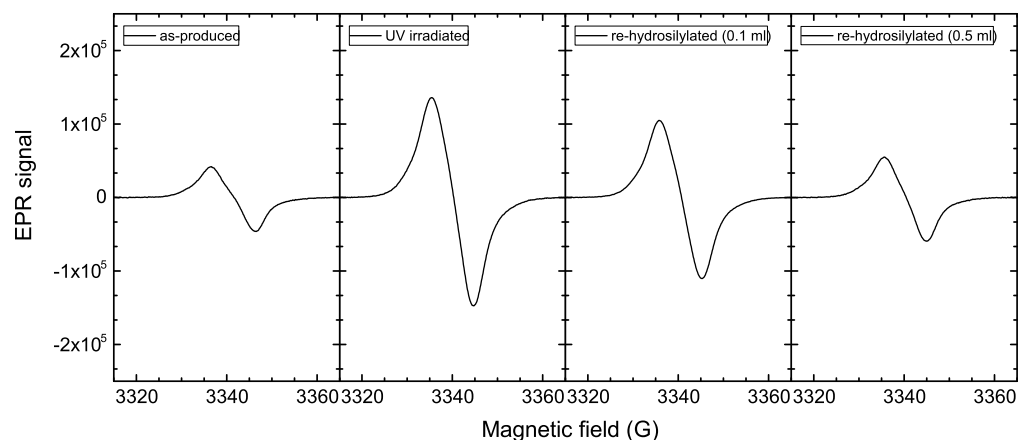


Fig. 7 EPR spectra of UV irradiated SiNCs after second thermal hydrosilylation with 0.1 ml and 0.5 ml of 1-dodecene.

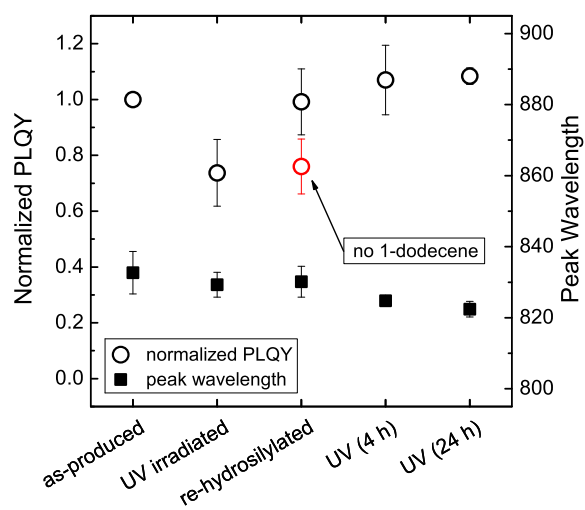


Fig. 8 PLQY recovery of SiQDs after second thermal hydrosilylation with 1-dodecene (open circles). Further UV irradiation saw no decrease in PLQY. No recovery was observed when heated in the absence of 1-dodecene (red). The peak PL wavelengths are represented by the solid squares.

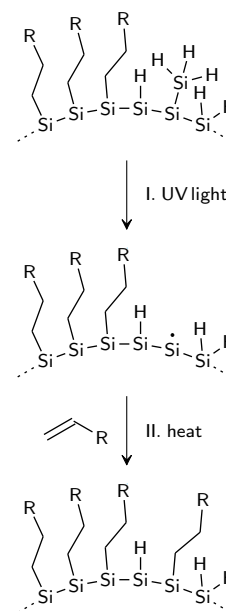
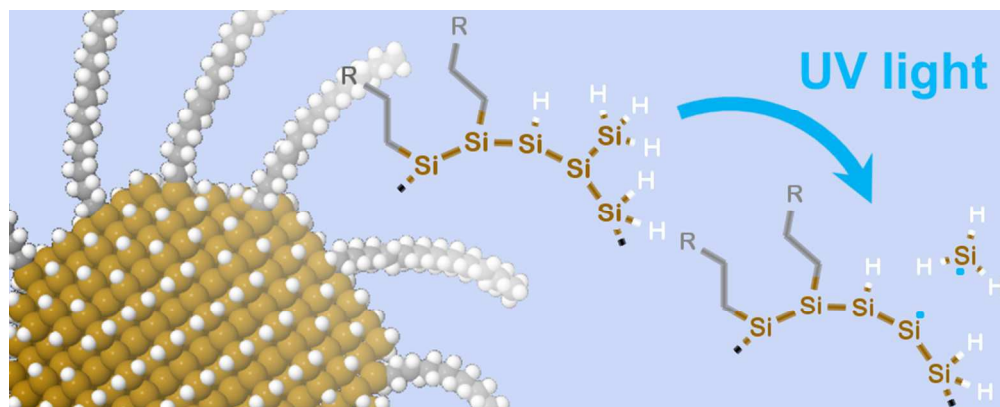


Fig. 9 Summary of the photodegradation and recovery process. I. Irradiation of the SiNCs with UV light results in the cleavage of weaker silicon hydrides from the surface. II. Hydrosilylation of the photobleached SiNCs with 1-dodecene passivates the surface defects and leads to recovery of the SiNCs' PLQY.

- Chem. Soc.*, 2010, **132**, 4048 – 4049.
- 28 L. A. Huck and J. M. Buriak, *J. Am. Chem. Soc.*, 2012, **134**, 489 – 497.
- 29 A. Kolodziej, *Opto-electronics Rev.*, 2004, **12**, 21 – 32.
- 30 E. Roduner, *Chem. Soc. Rev.*, 2006, **35**, 583 – 592.
- 31 A. B. Sieval, B. van den Hout, H. Zuilhof and E. J. Sudholter, *Langmuir*, 2001, **17**, 2172 – 2181.
- 32 J. Holm and J. T. Roberts, *Langmuir*, 2007, **23**, 11217 – 11224.
- 33 M. Niwano, M. Terashi and J. Kuge, *Surf. Sci.*, 1999, **420**, 6 – 16.
- 34 P. Gupta, V. Colvin and S. George, *Phys. Rev. B*, 1988, **37**, 8234 – 8243.
- 35 S. King, R. Davis and R. Nemanich, *Surf. Sci.*, 2009, **603**, 3104 – 3118.
- 36 R. Walsh, *Acc. Chem. Res.*, 1981, **1537**, 246 – 252.
- 37 J. Kanabus-Kaminska, J. Hawari, D. Griller and C. Chatgililoglu, *J. Am. Chem. Soc.*, 1987, **109**, 5268 – 5270.
- 38 D. Marra, E. Edelberg, R. Naone and E. Aydil, *J. Vac. Sci. Technol. A Vacuum, Surfaces, Film.*, 1998, **16**, 3199 – 3210.
- 39 J. J. Boland, *Surf. Sci.*, 1992, **261**, 17 – 28.
- 40 W. Beyer, *J. Appl. Phys.*, 1982, **53**, 8745 – 8750.
- 41 M. Wise, B. Koehler, P. Gupta, P. Coon and S. George, *Surf. Sci.*, 1991, **258**, 166 – 176.
- 42 A. Pusel, U. Wetterauer and P. Hess, *Phys. Rev. Lett.*, 1998, **81**, 645 – 648.



169x67mm (150 x 150 DPI)